

ARTICLE

Received 21 Feb 2013 | Accepted 19 Jul 2013 | Published 16 Aug 2013

DOI: 10.1038/ncomms3331

Thermodynamic behaviour of supercritical matter

Dima Bolmatov¹, V.V. Brazhkin² & K. Trachenko^{1,3}

Since their discovery in 1822, supercritical fluids have been of enduring interest and have started to be deployed in many important applications. Theoretical understanding of the supercritical state is lacking and is seen to limit further industrial deployment. Here we study thermodynamic properties of the supercritical state and discover that specific heat shows a crossover between two different regimes, an unexpected result in view of currently perceived homogeneity of supercritical state in terms of physical properties. We subsequently formulate a theory of system thermodynamics above the crossover, and find good agreement between calculated and experimental specific heat with no free-fitting parameters. In this theory, energy and heat capacity are governed by the minimal length of the longitudinal mode in the system only, and do not explicitly depend on system-specific structure and interactions. We derive a power law and analyse supercritical scaling exponents in the system above the Frenkel line.

¹School of Physics and Astronomy, Queen Mary University of London, Mile End Road, London E1 4NS, UK. ²Institute for High Pressure Physics, RAS, Moscow 142190, Russia. ³South East Physics Network. Correspondence and requests for materials should be addressed to D.B. (email: d.bolmatov@qmul.ac.uk).

Statistical mechanics is the art of predicting the behaviour of a system with a large number of degrees of freedom, given the laws governing its microscopic behaviour. The statistical description of liquids, in comparison with the solid and gas phases, is incomplete. The problem of formulating a rigorous mathematical description of liquids has always been regarded as much more difficult than that of the kinetic theory of gases or solid-state theory, stimulating the ongoing research^{1–9}. Owing to the simultaneous presence of strong interactions and large atomic displacements, common models and approximations used for gases and solids do not apply to liquids. For this reason, liquids do not generally fall into any simple classification and have been mostly treated as general many-body systems as a result.

In recent years, a significant effort has been devoted to investigation of various properties of supercritical fluids^{10–14}. This has been an exciting field with a long history since 1822 when Baron Charles Cagniard de la Tour discovered supercritical fluids while conducting experiments involving the discontinuities of the sound in a sealed cannon barrel filled with various fluids at high temperature¹⁵. More recently, supercritical fluids have started to be deployed in several important applications, ranging from the extraction of floral fragrance from flowers to applications in food science, such as creating decaffeinated coffee, functional food ingredients, pharmaceuticals, cosmetics, polymers, powders, bio- and functional materials, nano-systems, natural products, biotechnology, fossil and bio-fuels, microelectronics, energy and environment^{13,14,16}. Much of the excitement and interest of the past decade is because of the enormous progress made in increasing the power of relevant experimental tools^{17–20}. The development of new experimental methods and improvement of existing ones continues to have an important role in this field^{22–26}, with recent research focusing on dynamic properties of fluids^{27–32}.

High density and high thermal motion are two main properties responsible for efficient cleaning, dissolving and extracting abilities of supercritical fluids in the above industrial applications. From the point of view of practical applications, supercritical fluids have got the best of both worlds: high density comparable to ordinary liquids and solids, and high thermal motion and diffusivity approaching that of gases. Notably, it is this very combination that presents a formidable problem to the theory: high density and strong interactions mean that theories and approximations used for dilute gases do not apply³³. Enskog's³³ and related early kinetic approaches to gases were followed by more extensive developments, yet they do not adequately describe dense systems with strong interactions and many-body correlations, such as supercritical fluids. One general issue with extending gas-like approaches to fluids was noted earlier: in a system with strong interactions, the system energy strongly depends on the type of interactions, and is therefore system-specific, ruling out the possibility to develop a theory that is universally applicable to many fluids, in contrast to gases and solids³⁴.

In addition to theoretical challenges, the lack of fundamental understanding is seen as an obstacle towards wider deployment of supercritical fluids in industrial applications, primarily because of the absence of guidance regarding pressure and temperature at which the desired properties are optimized, as well as the possibility to use new systems¹³.

In this paper, we focus on the thermodynamic properties of the supercritical state. On the basis of molecular dynamics simulations, we find that specific heat shows a crossover between two different dynamic regimes of the low-temperature rigid liquid and high-temperature non-rigid gas-like fluid. The crossover challenges the currently held belief that no difference can be made between a gas and a liquid above the critical point, and that

the supercritical state is homogeneous in terms of physical properties³⁵. We subsequently formulate a theory of system thermodynamics and heat capacity above the crossover. In this theory, energy and heat capacity are governed by the minimal length of the longitudinal mode in the system only, and do not depend on system-specific structure and interactions. We further study the predicted relationship between supercritical exponents of heat capacity and viscosity. A good agreement is demonstrated between calculated and experimental data for noble and molecular supercritical fluids with no free-fitting parameters.

Results

Dynamic crossover of the specific heat. We start with molecular dynamics simulations of a model liquid. Our primary aim here is to show that specific heat, c_V , shows a crossover in the supercritical region of the phase diagram. This result is unexpected in view of currently perceived homogeneity of supercritical state in terms of physical properties.

Using molecular dynamics simulations (see Methods), we have simulated the binary Lennard-Jones (LJ) fluid. We have simulated the system with 64,000 atoms using constant-volume (nve) ensemble in the wide temperature range (see Fig. 1) well extending into the supercritical region. Indeed, the temperature range in Fig. 1 is between about $2T_c$ and $70T_c$, where T_c is the critical temperature of Ar, $T_c \approx 150$ K; the simulated density, $2,072 \text{ kg m}^{-3}$, corresponds to approximately four times the critical density of Ar. From the energy of the system E at each temperature, we calculate constant-volume specific heat, c_V , as $c_V = (1/N)(dE/dT)$ ($k_B = 1$).

We observe that c_V decreases steeply from the solid-state value of about $3k_B$ at low temperature to $\sim 2k_B$ around 2,000 K. The steep decrease is followed by crossing over to a considerably weaker temperature dependence. This crossover is a new effect not reported in previous molecular dynamics (MD) simulations. We further observe that the crossover takes place around $c_V \approx 2k_B$. This value of $c_V = 2k_B$ is non-coincidental and corresponds to the crossover taking place across the Frenkel line^{36,37} as discussed below.

Crossing the Frenkel line corresponds to the qualitative change of atomic dynamics in a liquid. In liquids, atomic motion has two components: a solid-like, quasi-harmonic vibrational motion about equilibrium locations and diffusive gas-like jumps between neighbouring equilibrium positions. As the temperature increases, a particle spends less time vibrating and more time

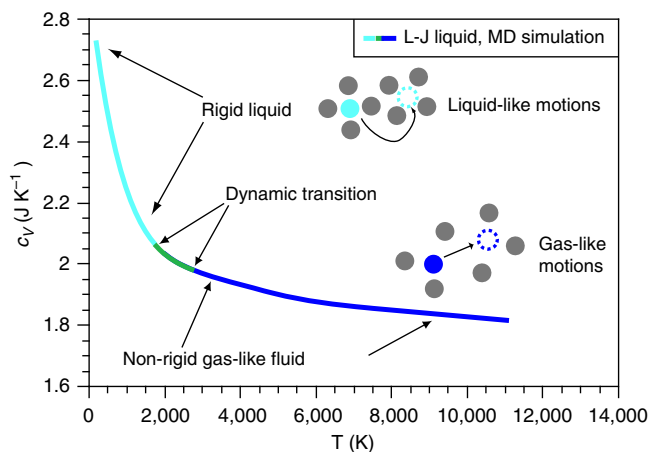


Figure 1 | Heat capacity of binary LJ fluid. Calculated c_V showing the crossover and continuous dynamical transition around $c_V \approx 2$, ($k_B = 1$). The crossover takes place between different dynamical regimes of the rigid liquid and non-rigid supercritical fluid.

diffusing. Eventually, the solid-like oscillating component of motion disappears; all that remains is the gas-like ballistic motion. That disappearance, a qualitative change in particle dynamics, corresponds to crossing the Frenkel line, the transition of the substance from the liquid dynamics to the gas dynamics. This transition takes place when liquid relaxation time τ (τ is liquid relaxation time, the average time between consecutive atomic jumps at one point in space³⁸) approaches its minimal value, τ_D , the Debye vibration period. As recently discussed^{36,37}, crossing the Frenkel line is accompanied by qualitative changes of most important properties of the system, including diffusion, viscosity, thermal conductivity and dispersion curves^{36,37}. One of these properties is the crossover of the speed of sound and appearance of the high-frequency ‘fast’ sound^{20,39–41}. At the microscopic level, the Frenkel line can be identified by the loss of oscillations in the velocity autocorrelation function³⁷, a point studied in detail elsewhere.

Figure 1 implies that in addition to the dynamic properties discussed above, the thermodynamics of the system changes at the Frenkel line too. This is an important general insight regarding the behaviour of the supercritical state.

The initial steep decrease of c_V from about $3k_B$ to $2k_B$ can be quantitatively explained by the progressive loss of two transverse waves with frequency $\omega > 1/\tau$ (refs 42–44). Physically, this picture is based on Frenkel’s prediction that on timescale shorter than τ , liquid is a solid, and therefore supports rigidity and solid-like transverse waves at short times or at frequency larger than $\omega > 1/\tau$ (ref. 45). When τ approaches its maximal value, τ_D , the liquid can not sustain transverse waves at any frequency⁴⁶. Consequently, the potential energy of the system is due to the longitudinal mode only, giving the total energy of $2NT$ and specific heat of $2k_B$ ^{42,44}. Hence, the decrease of c_V from about $3k_B$ to $2k_B$ corresponds to the region of a ‘rigid’ liquid, where short-time solid-like rigidity and high-frequency transverse waves exist. On the other hand, the liquid is unable to sustain transverse waves at any available frequency above the Frenkel line. Instead, the liquid enters a new dynamic ‘non-rigid’ gas-like regime, where oscillatory component of particles is lost and the motion becomes purely collisional as in a gas.

We therefore need to develop a new theory capable of describing thermodynamics of supercritical matter above the Frenkel line, where the system enters the new dynamic regime and where c_V falls below $2k_B$ and approaches the ideal-gas value of $3/2k_B$ at high temperature (see Fig. 1).

Thermodynamic theory of supercritical state. We now focus on the theory of the non-rigid gas-like liquid above the Frenkel line, and add a new proposal regarding how the system energy can be evaluated. As temperature rises in the ballistic gas-like regime and kinetic energy increases, the mean free path l , the average distance between particle collisions, increases. At the Frenkel line where the ballistic regime starts, l is comparable to interatomic separation. In the limit of high temperature where the particle’s kinetic energy is much larger than potential energy, l tends to infinity as in the non-interacting ideal gas. Our proposal is that l determines the shortest wavelength of the longitudinal mode that exists in the system, λ , because below this length the motion is purely ballistic and therefore can not be oscillatory, $\lambda = l$. On the other hand, the longitudinal modes with larger wavelength are supported and they represent the excitations existing in the supercritical system.

We note that the existence of long-wavelength longitudinal waves in a gas (sound) is well known. What is new here is that we propose that the contribution of the longitudinal waves to the energy of the gas-like supercritical system starts from very short

wavelengths comparable to interatomic separation a . In this sense, we are extending the solid-state concepts (for example, short-wavelength solid-like phonons with Debye density of states, see below) to the new area of gas-like supercritical state, where these ideas have not been hitherto contemplated. Indeed, it is well established experimentally that dynamics in subcritical liquids shows solid-like character, in that liquids can sustain high-frequency propagating modes down to wavelengths on the atomic scale, with solid-like dispersion relations⁴⁶. Importantly, recent experimental evidence shows that the same applies to supercritical fluids^{20,47}.

Here and elsewhere, our discussion of liquid vibrational states includes an important point. Namely, a disordered system, such as glass or liquid, supports non-decaying collective excitations obtainable from the secular equation involving the force matrix constructed from the amorphous glass or liquid structure. Harmonic plane waves naturally decay in liquids as in any non-crystalline systems, yet importantly they are clearly seen in fluids experimentally as quasi-linear solid-like dispersion relations even in low-viscous liquids^{26,46,48}, leading to the quadratic density of states $g(\omega) \propto \omega^2$. A detailed discussion of this point is forthcoming.

In the proposed theory, the energy of the non-rigid supercritical fluid per particle includes the contribution from the kinetic energy, $K = \frac{3}{2}k_B T$, and the potential energy of the longitudinal phonons with wavelengths larger than l . Using the equipartition theorem $\langle P_i \rangle = \langle E_i \rangle / 2$, where $\langle E_i \rangle$ is the energy of the longitudinal phonons, we write

$$E = \frac{3}{2}k_B T + \frac{1}{2} \int_0^{\omega_0} \varepsilon(\omega, T) g(\omega) d\omega + E_{\text{anh}} \quad (1)$$

where the upper integration limit ω_0 is given by the shortest wavelength in the system, λ : $\omega_0 = (2\pi/\lambda)c$, c is the speed of sound, $\varepsilon(\omega, T)$ is the mean energy of harmonic oscillator, $\varepsilon(\omega, T) = \hbar\omega/2 + \hbar\omega/(e^{\hbar\omega/T} - 1)$, or $\varepsilon(T) = k_B T$ is the classical case and E_{anh} is the anharmonic contribution to the phonon energy.

The second term in equation (1) can be calculated using the Debye density of states, $g(\omega) \equiv 3/\omega_D^3(\omega^2)$, giving $k_B T(\omega^3/\omega_D^3)$, or $k_B T(a^3/\lambda^3)$, where a is the interatomic separation. The use of the quadratic density of states is supported by the experimental evidence showing solid-like quasi-linear dispersion relationships in supercritical fluids^{20,47} similar to the subcritical liquids. E_{anh} can be evaluated in the Grüneisen approximation from the softening of phonon frequencies with temperature, with the result that the energy is modified as $E \rightarrow E(1 + \alpha T/2)$, where α is the coefficient of thermal expansion^{43,44}. Then, the energy of non-rigid gas-like supercritical fluid becomes:

$$E = \frac{3}{2}k_B T + \left(1 + \frac{1}{2}\alpha T\right) \frac{1}{2}k_B T \frac{a^3}{\lambda^3} \quad (2)$$

We observe that when $\lambda \approx a$ at the Frenkel line, equation (2) gives $E = 2k_B T$ and the specific heat of 2 (here we neglect the small term αT). This corresponds to the crossover of c_V in Fig. 1 to the gas-like regime as discussed above. When λ increases on temperature increase in the gas-like regime, equation (2) predicts that c_V tends to $3/2$, the ideal-gas value as expected.

Comparison with experimental data. As discussed above, λ is given by the particle mean free path in the non-rigid gas-like regime, and can therefore be calculated from $\eta = \frac{1}{3}\rho\bar{u}\lambda$, where η is viscosity, ρ is density and \bar{u} is average velocity. Therefore, equation (2) provides an important relationship between the energy of the non-rigid supercritical liquid and its gas-like

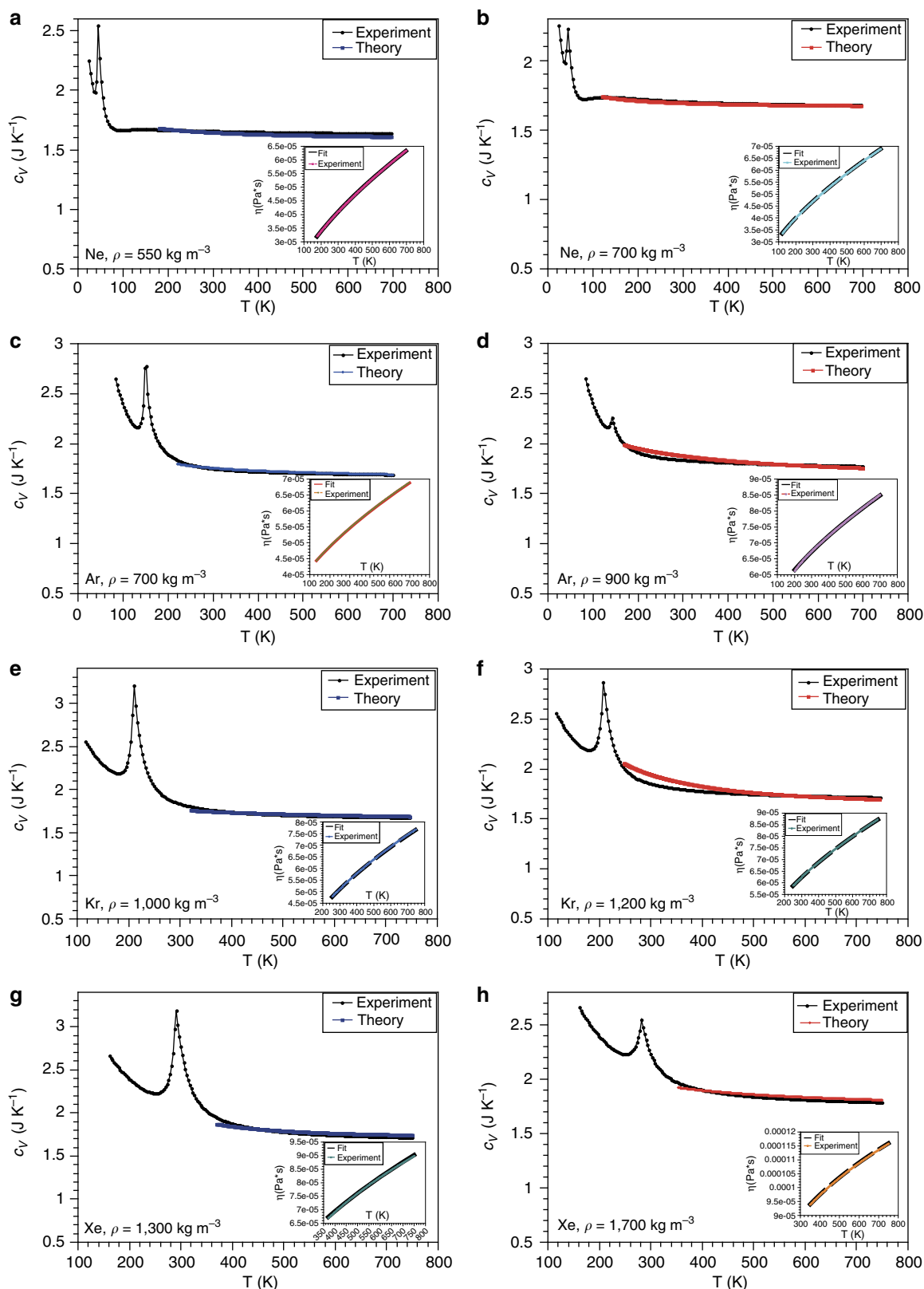


Figure 2 | Heat capacity of noble gas liquids. Experimental and calculated c_V ($k_B = 1$) for noble non-rigid supercritical fluids. Experimental c_V and η are taken from the NIST database at different densities as shown in the Figure (a–h). Values of α used in the calculation are $3.5 \times 10^{-3} \text{ K}^{-1}$ (Ne), $3.3 \times 10^{-3} \text{ K}^{-1}$ (Ar), $1.8 \times 10^{-3} \text{ K}^{-1}$ (Kr) and $8.2 \times 10^{-4} \text{ K}^{-1}$ (Xe). The uncertainty of both experimental heat capacities and viscosities is about 2–5%. Insets show viscosity fits.

viscosity. We now check this relationship experimentally by comparing the specific heat $c_V = dE/dT$ predicted by equation (2) and the experimental c_V .

We have used the National Institute of Standards and Technology (NIST Chemistry WebBook, <http://webbook.nist.gov/chemistry/fluid>) database. We aimed to check our theoretical

predictions and selected the isochoric data of several supercritical noble and molecular liquids in a wide range of temperature and density. We note that λ in equation (1) changes in response to both temperature and density: λ increases with temperature and decreases with density. Practically, the range of isochoric data in the NIST database is fairly narrow in terms of density compared with the range of temperature. We therefore analyse the temperature behaviour of c_V and η along several isochores. Our choice of liquids is dictated by the availability of isochoric data in the supercritical region. For each density, we fit experimental viscosity to $\eta = A_0 + A_1 T^{\alpha}$, calculate λ from $\eta = \frac{1}{3} \rho \bar{u} \lambda$ and subsequently use λ in equation (2) to calculate c_V .

We note that Debye model is not a good approximation in molecular liquids, where the frequency of intra-molecular vibrations considerably exceeds the rest of frequencies in the system (3340 K in N_2 and 3572 K in CO). However, the intra-molecular modes are not excited in the temperature range of experimental c_V (see Figs 2 and 3). Therefore, the contribution of intra-molecular motion to c_V is purely rotational, c^{rot} . On the other hand, the rotational motion is excited in the considered temperature range, and is therefore classical, giving $c^{rot} = R$ for linear molecules in N_2 and CO. Consequently, c_V for molecular liquids shown in Fig. 3 correspond to heat capacities per molecule, with c^{rot} subtracted from the experimental data.

We also note that experimental isochoric c_V is affected by λ -like critical anomalies (see Figs 2–4) because the isochoric NIST data do not extend far above the critical point. Here we do not consider critical effects related to phase transitions, and therefore fit the data at temperatures that are high enough to be affected by the λ -anomaly at the phase transition. In Figs 2–4 we observe good agreement between experimental and predicted c_V , in view of (a) 2–5% uncertainty of experimental c_V and η (see NIST Chemistry WebBook), (b) approximations introduced by the Debye model and (c) increased curvature of c_V at low temperature because of proximity of λ -anomalies that are not taken into account by the theory. Notably, the agreement is achieved without using free-fitting parameters because ρ , α , \bar{u} and a are fixed by system properties. Values of these parameters used in equation (1) are in good agreement with their experimental values.

Another way to compare our theory and experimental data is to study supercritical exponents of specific heat and viscosity. Indeed, if η in the non-rigid gas-like supercritical region can be approximated as a power law, $\eta \propto T^\alpha$, then equation (2) makes two predictions. First, E and c_V should also follow power laws. Second, equation (2) provides a specific relationship between the scaling exponents of η on one hand and E and c_V on the other hand, the relationship that we check below.

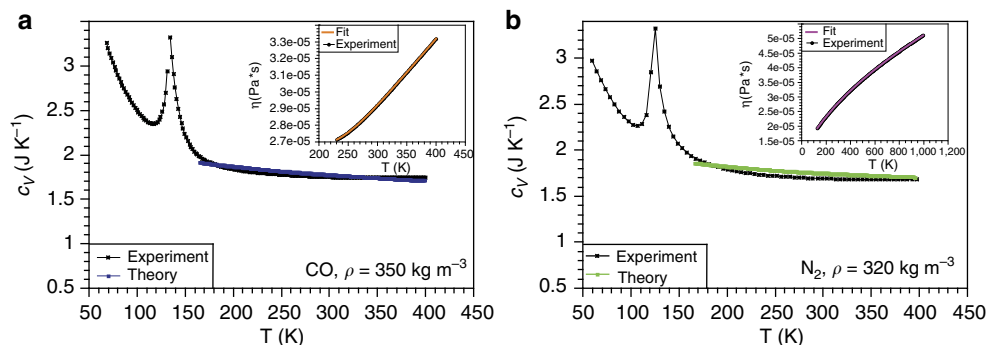


Figure 3 | Heat capacity of molecular liquids. Experimental and calculated c_V ($k_B = 1$) for molecular non-rigid supercritical fluids (a, b). Experimental c_V and η are taken from the NIST database. Values of α used in the calculation are $6.5 \times 10^{-3} \text{ K}^{-1}$ (CO) and $8.5 \times 10^{-3} \text{ K}^{-1}$ (N_2). The uncertainty of both experimental heat capacities and viscosities is about 2–5%. Insets show viscosity fits.

Apart from comparing theory and experiments, studying the supercritical scaling exponents is interesting in the wider context of scaling behaviour of physical properties. In the area of phase transitions, the scaling behaviour idea has been a crucial element in the subject of liquids and other systems from the nineteenth century onwards⁴⁹. Critical points occur in a great variety of systems^{50–53}, yet there is a considerable degree of similarity in the way in which systems approach the critical point⁵⁴. Here the calculation of critical exponents serves as one of the main test of the theories.

Once analysed within our theory below, experimental temperature dependence of η , \bar{u} , E and c_V (see NIST Chemistry WebBook) can be fairly well approximated by the power law above the Frenkel line. Therefore, we use the following power-law relationships:

$$\eta = \text{const} \times T^\alpha \quad (3)$$

$$\bar{u} = \text{const} \times T^{\frac{1}{2}} \quad (4)$$

$$E = 1.5 \times T + \text{const} \times T^\delta \quad (5)$$

$$c_V = 1.5 + \frac{\text{const}}{T^\xi} \quad (6)$$

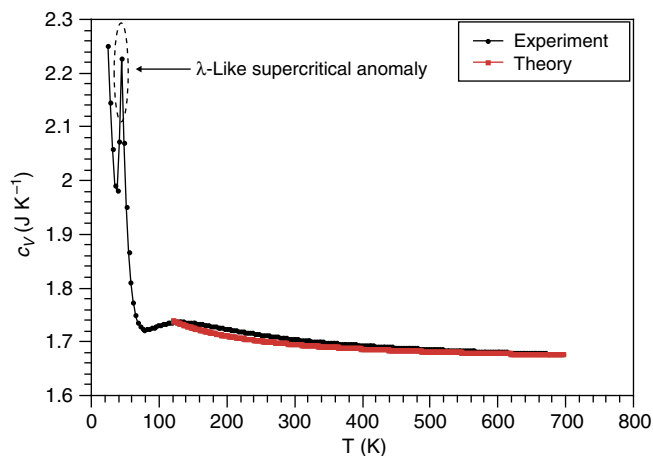


Figure 4 | Heat capacity of liquid Ne. Experimental and calculated c_V ($k_B = 1$) for non-rigid supercritical fluid Ne. Experimental c_V and η are taken from the NIST database at density 700 kg m^{-3} . Value of α used in the calculation is $3.5 \times 10^{-3} \text{ K}^{-1}$.

Table 1 | Comparison between experiment and theory.

Supercritical Fluid	$\langle \xi \rangle$	$\langle \gamma_{th} \rangle$	$\langle \gamma_{exp} \rangle$
Ar	0.17	0.56	0.55
Ne	0.17	0.56	0.64
Kr	0.18	0.56	0.60
Xe	0.18	0.56	0.55
CO	0.17	0.56	0.61
N ₂	0.27	0.59	0.59

Power-law exponents ξ , γ_{exp} and γ_{th} , averaged over different densities: Ne(600 kg m⁻³, 700 kg m⁻³, 900 kg m⁻³), Ar (700 kg m⁻³, 800 kg m⁻³, 900 kg m⁻³), Kr(1,100 kg m⁻³, 1,300 kg m⁻³, 1,500 kg m⁻³), Xe(1,300 kg m⁻³, 1,500 kg m⁻³, 1,700 kg m⁻³), CO(350 kg m⁻³) and N₂(320 kg m⁻³).

From $\eta = \frac{1}{3}\rho\bar{u}\lambda$ ($k_B = 1$), $\lambda = \text{const} \times T^\gamma - 0.5$. Using λ in equation (2) gives for the energy (neglecting the small term αT):

$$E \propto T^{2.5-3\gamma} \quad (7)$$

and specific heat:

$$c_V \propto (2.5 - 3\gamma)T^{1.5-3\gamma} \quad (8)$$

Then, from equations (3), (7) and (8), we find the following relationships between the power-law scaling exponents:

$$2.5 - 3\gamma = \delta \quad (9)$$

$$3\gamma - 1.5 = \xi \quad (10)$$

We note that equations (7) and (8), together with the general requirement for c_V to be positive and the experimental requirement for c_V to decrease with temperature, imply that γ should be in the range $\frac{1}{2} < \gamma < \frac{5}{6}$. This is the case for the experimental data we examined, as will be shown below. We also note that $\gamma = \frac{1}{2}$ corresponds to the non-interacting ideal gas and $\eta \propto T^{0.5}$.

We now check equation (10) experimentally. Using the NIST database and equation (6), we calculate ξ from the slope of $\log(c_V = -1.5)$ vs. $\log(1/(T - T_F))$, where T_F corresponds to the temperature on the Frenkel line and 1.5 is the asymptotic gas value of specific heat. Using equation (10), we calculate the predicted theoretical value γ_{th} and compare it with the experimental γ_{exp} obtained from fitting the experimental viscosity to $\eta \propto T^{\gamma_{exp}}$.

In Table 1, we show ξ , γ_{exp} and γ_{th} , averaged over several data sets taken along the isochores at several different densities. We observe the overall good agreement between γ_{exp} and γ_{th} . We further observe that the power exponent of specific heat, ξ , is close to 0.2 for different systems. In our theory, the similarity of temperature behaviour of c_V is due to temperature dependence of λ . This point is discussed in the next section in more detail.

Discussion

Our first important observation in this work is that contrary to the current belief, the thermodynamic properties of the supercritical state are not homogeneous. Instead, the specific heat shows a crossover related to the change of particle dynamics, which we attributed to the recently introduced Frenkel line.

We have subsequently focused on thermodynamic properties of supercritical fluids above the Frenkel line. Here, we faced the problem of strong interactions, the long-persisting challenge in condensed matter physics. Indeed, strong interactions imply that approximations used for dilute gases do not apply to real dense liquids³³. If we consider realistic strong interactions (assuming that interactions are known and can be represented in analytical form, the assumption that is valid for a relatively small number of

simple systems only) and structural correlations that often include those beyond two-body correlations, we quickly find that the problem becomes intractable. Further, strong interactions, coupled with their specificity in different systems, have been suggested to preclude the calculation of energy and heat capacity in general form from the outset³⁴.

In this paper, we addressed the problem in a different way, by substituting all potentially complicated effects of interactions and structural correlations by one physical quantity, the minimal wavelength of the longitudinal mode in the system λ . This has enabled us to rationalize the experimental behaviour of c_V as well as to provide the relationship between different physical properties and experimental outcomes (for example, relationship between c_V and η). Notably, our approach unveils similarity of thermodynamics of supercritical state in the following sense. First, c_V does not explicitly depend on system details such as structure and interactions, but on λ only. Fluids may have very different structure and interactions, yet our theory predicts the similarity of their thermodynamic behaviour as long as λ behaves similarly in those systems. Second, and more specifically, our approach predicts that supercritical scaling of thermodynamic properties, such as heat capacity, is governed by viscosity scaling. Consequently, similar temperature scaling of viscosity gives similar temperature scaling of thermodynamic properties. We note here that we have mostly dealt with systems with fairly simple interatomic interactions, whereas the found similarity of thermodynamic behaviour may not hold in systems with the hierarchy of interactions and non-trivial structural transformations such as water⁵⁵.

Methods

Molecular dynamics. We have used DL-POLY molecular dynamics simulation code⁵⁶ to run the system with 64,000 atoms in the constant-volume (nve) ensemble at different temperatures. We have used 3,000 processors of the high-throughput cluster to simulate 500 temperature points in the temperature range of about 0–12,000 K shown in Fig. 1. We have used the model LJ potential⁵⁷ to simulate model liquids. Each structure was equilibrated for 25 ps, and the system energy and other properties were averaged for the following 25 ps of the production run. The timestep of 0.001 ps was used.

References

- Angell, C. A. Insights into phases of liquid water from study of its unusual glass-forming properties. *Science* **319**, 582–587 (2008).
- Kivelson, S. A. & Tarjus, G. In search of a theory of supercooled liquids. *Nat. Mater.* **7**, 831–833 (2008).
- Widmer-Cooper, A., Perry, H., Harrowell, P. & Reichman, D. R. Irreversible reorganization in a supercooled liquid originates from localized soft modes. *Nat. Phys.* **4**, 711–715 (2008).
- Stevenson, J. D., Schmalian, J. & Wolynes, P. G. The shapes of cooperatively rearranging regions in glass-forming liquids. *Nat. Phys.* **2**, 268–274 (2006).
- Biroli, G., Bouchaud, J.-P., Cavagna, A., Grigera, T. S. & Verrocchio, P. Thermodynamic signature of growing amorphous order in glass-forming liquids. *Nat. Phys.* **4**, 771–775 (2008).
- Gundermann, D. *et al.* Predicting the density-scaling exponent of a glass-forming liquid from Prigogine-Defay ratio measurements. *Nat. Phys.* **7**, 816–821 (2011).
- Larini, L., Ottocian, A., Michele, C. De & Leporini, D. Universal scaling between structural relaxation and vibrational dynamics in glass-forming liquids and polymers. *Nat. Phys.* **4**, 42–45 (2008).
- Bolmatov, D. Equations of state for simple liquids from the Gaussian equivalent representation method. *J. Stat. Phys.* **137**, 765–773 (2009).
- Mauro, J. C., Yue, Y., Ellison, A. J., Gupta, P. K. & Allan, D. C. Viscosity of glass-forming liquids. *Proc. Natl Acad. Sci. USA* **106**, 19780–19784 (2009).
- Cowan, J. & Cann, J. Supercritical two-phase separation of hydrothermal fluids in the Troodos ophiolite. *Nature* **333**, 259–261 (1988).
- Eckert, C. A., Knutson, B. L. & Debenedetti, P. G. Supercritical fluids as solvents for chemical and materials processing. *Nature* **383**, 313–318 (1996).
- Kessel, R., Schmidt, M. W., Ulmer, P. & Pettke, T. Trace element signature of subduction-zone fluids, melts and supercritical liquids at 120–180 km depth. *Nature* **437**, 724–727 (2005).

13. Kiran, E., Debenedetti, P. G. & Peters, C. J. *Supercritical Fluids: Fundamentals and Applications*, NATO Science Series E: Applied Sciences 366 (Boston, Kluwer Academic Publishers, 2000).
14. McHardy, J. & Sawan, S. P. *Supercritical Fluid Cleaning: Fundamentals, Technology and Applications* (Westwood, Noyes Publications, 1998).
15. Berche, B., Henkel, M. & Kenna, R. Critical phenomena: 150 years since Cagniard de la Tour. *J. Phys. Studies* **13**, 3201–3209 (2009).
16. Brunner, G. Applications of supercritical fluids. *Annu. Rev. Chem. Biomol. Eng.* **1**, 321–342 (2010).
17. De Simone, J. M. Practical approaches to green solvents. *Science* **296**, 799–803 (2002).
18. Pai, R. A. *et al.* Mesoporous silicates prepared using preorganized templates in supercritical fluids. *Science* **303**, 507–510 (2004).
19. Johnston, K. P. & Shah, P. S. Making nanoscale materials with supercritical fluids. *Science* **303**, 482–483 (2004).
20. Simeoni, G. G. *et al.* The Widom line as the crossover between liquid-like and gas-like behaviour in supercritical fluids. *Nat. Phys.* **6**, 503–507 (2010).
21. Sette, F., Krisch, M. H., Masciocvecchio, C., Ruocco, G. & Monaco, G. Dynamics of glasses and glass-forming liquids studied by inelastic X-ray scattering. *Science* **280**, 1550–1555 (1998).
22. Fecko, C. J., Eaves, J. D., Loparo, J. J., Tokmakoff, A. & Geissler, P. L. Ultrafast hydrogen-bond dynamics in the infrared spectroscopy of water. *Science* **301**, 1698–1702 (2003).
23. Siwick, B. J., Dwyer, J. R., Jordan, R. E. & Miller, R. J. D. An atomic-level view of melting using femtosecond electron diffraction. *Science* **302**, 1382–1385 (2003).
24. Whitesides, G. M. The origins and the future of microfluidics. *Nature* **442**, 368–373 (2006).
25. McMillan, P. F. & Stanley, H. E. Fluid phases: Going supercritical. *Nat. Phys.* **6**, 479–480 (2010).
26. Giordano, V. M. & Monaco, G. Fingerprints of order and disorder on the high-frequency dynamics of liquids. *Proc. Natl Acad. Sci. USA* **107**, 21985–21989 (2010).
27. Fradin, C. *et al.* Reduction in the surface energy of liquid interfaces at short length scales. *Nature* **403**, 871–874 (2000).
28. Berthier, L. *et al.* Direct experimental evidence of a growing length scale accompanying the glass transition. *Science* **310**, 1797–1800 (2005).
29. Salmon, P. S., Martin, R. A., Mason, P. E. & Cuello, G. J. Topological versus chemical ordering in network glasses at intermediate and extended length scales. *Nature* **435**, 75–78 (2005).
30. Royall, C. P., Aarts, D. G. A. L. & Tanaka, H. Bridging length scales in colloidal liquids and interfaces from near-critical divergence to single particles. *Nat. Phys.* **3**, 636–640 (2007).
31. Karmakar, S., Dasgupta, S. & Sastry, S. Growing length and time scales in glass-forming liquids. *Proc. Natl Acad. Sci. USA* **106**, 3675–3679 (2009).
32. Flenner, E. & Szamel, G. Characterizing dynamic length scales in glass-forming liquids. *Nat. Phys.* **8**, 696–697 (2012).
33. Chapman, S. & Enskog, T. G. *The Mathematical Theory of Non-Uniform Gases* (Cambridge University Press, 1995).
34. Landau, L. D. & Lifshitz, L. D. *Statistical Physics* (Nauka, Moscow, Russia, 1964).
35. Barrat, J. L. & Hansen, J. P. *Basic Concepts for Simple and Complex Liquids* (Cambridge, Cambridge University Press, 2003).
36. Brazhkin, V. V. & Trachenko, K. What separates a liquid from a gas. *Phys. Today* **65**, 68 (2012).
37. Brazhkin, V. V., Fomin, Yu. D., Lyapin, A. G., Ryzhov, V. N. & Trachenko, K. Two liquid states of matter: A dynamic line on a phase diagram. *Phys. Rev. E* **85**, 031203 (2012).
38. Frenkel, J. *Kinetic Theory of Liquids* (eds Fowler, R. H., Kapitza, P. & Mott, N. F.) (New York, Oxford University Press, 1947).
39. Gorelli, F. *et al.* Liquidlike behavior of supercritical fluids. *Phys. Rev. Lett.* **97**, 245702 (2006).
40. Bencivenga, F. *et al.* Structural and collisional relaxations in liquids and supercritical fluids. *Phys. Rev. Lett.* **98**, 085501 (2007).
41. Bencivenga, F. *et al.* Adiabatic and isothermal sound waves: The case of supercritical nitrogen. *Europhys. Lett.* **75**, 70–76 (2006).
42. Bolmatov, D., Brazhkin, V. V. & Trachenko, K. The phonon theory of liquid thermodynamics. *Sci. Rep.* **2**, 421 (2012).
43. Trachenko, K. & Brazhkin, V. V. Heat capacity at the glass transition. *Phys. Rev. B* **83**, 014201 (2011).
44. Bolmatov, D. & Trachenko, K. Liquid heat capacity in the approach from the solid state: Anharmonic theory. *Phys. Rev. B* **84**, 054106 (2011).
45. Bolmatov, D., Brazhkin, V. V. & Trachenko, K. Helium at elevated pressures: quantum liquid with non-static shear rigidity. *J. Appl. Phys.* **113**, 103514 (2013).
46. Pilgrim, W. C. & Morkel, C. State dependent particle dynamics in liquid alkali metals. *J. Phys. Condens. Matter* **18**, R585 (2006).
47. Cunsolo, H. E. *et al.* Microscopic relaxation in supercritical and liquid neon. *J. Chem. Phys.* **114**, 2259–2267 (2001).
48. Hosokawa, S., Inui, M. & Kajihara, Y. *et al.* Transverse acoustic excitations in liquid Ga. *Phys. Rev. Lett.* **102**, 105502 (2009).
49. Stanley, H. E. Scaling, universality, and renormalization: three pillars of modern critical phenomena. *Rev. Mod. Phys.* **71**, S358 (1999).
50. Mishima, O. & Suzuki, Y. Propagation of the polyamorphic transition of ice and the liquid-liquid critical point. *Nature* **419**, 599–603 (2002).
51. Senthil, T. *et al.* Quantum critical points. *Science* **303**, 1490–1494 (2004).
52. Elmatad, Y. S., Jack, R. L., Chandler, D. & Garrahan, J. P. Finite-temperature critical point of a glass transition. *Proc. Natl Acad. Sci. USA* **107**, 12793–12798 (2010).
53. Tanaka, H., Kawasaki, T., Shintani, H. & Watanabe, K. Critical-like behaviour of glass-forming liquids. *Nat. Mater.* **9**, 324–331 (2010).
54. Holten, V. & Anisimov, M. A. Entropy-driven liquid-liquid separation in supercooled water. *Sci. Rep.* **2**, 713 (2012).
55. Skinner, L. B. *et al.* Benchmark oxygen-oxygen pair-distribution function of ambient water from x-ray diffraction measurements with a wide Q-range. *J. Chem. Phys.* **138**, 074506 (2013).
56. Todorov, I. T., Smith, B., Dove, M. T. & Trachenko, K. DL-POLY-3: new dimensions in molecular dynamics simulations via massive parallelism. *J. Mater. Chem.* **16**, 1911–1119 (2006).
57. Kob, W. & Andersen, H. C. Scaling behavior in the β -relaxation regime of a supercooled Lennard-Jones mixture. *Phys. Rev. Lett.* **73**, 1376 (1994).

Acknowledgements

D.B. is thankful to Myerscough Bequest and K.T. is thankful to EPSRC for the financial support. D.B. acknowledges Thomas Young Centre for Junior Research Fellowship and Cornell University (Neil Ashcroft and Roald Hoffmann) for hospitality. V.B. is grateful to RFBR (11-02-00303; 13-02-12008) for the financial support.

Author contributions

All authors have contributed equally to this work.

Additional information

Competing financial interests: The authors declare no competing financial interests.

Reprints and permission information is available online at <http://npg.nature.com/reprintsandpermissions/>

How to cite this article: Bolmatov, D. *et al.* Thermodynamic behaviour of supercritical matter. *Nat. Commun.* 4:2331 doi: 10.1038/ncomms3331 (2013).